MAGNETOHYDRODYNAMIC METHOD OF GENERATING SOLITARY WAVES

Yu. B. Kolesnikov and V. A. Miroshnikov

UDC 537.84

For the generation of solitary waves we usually employ two methods. According to the first method [1, 2], the waves are formed with the aid of a piston mounted near the end wall of a rectangular channel. The piston is propelled sharply in a direction parallel to the end wall. With the second method [3, 4] a thin barrier is installed at the inlet portion to the channel. On either side of this barrier two different fluid levels are established. The solitary waves are formed when the barrier is suddenly removed. Sudden displacements of the barrier or piston lead to significant perturbations in the original fluid-surface profile. Of interest is a method which allows us significantly to reduce these perturbations. In the present study we propose precisely such a method, based on the MHD effects in weakly conducting media.

The Generation Method

The formation of an initial free-surface fluid profile is illustrated in Fig. 1. A channel fabricated out of Plexiglas exhibits a rectangular cross section with a width of 30 mm, a height of 65 mm, and a length of $L_0 = 550$ mm. Two thin flat electrodes, fabricated of stainless steel, were mounted at the side walls of the channel. The electrodes were 0.5 mm in thickness, and 10 mm in width. The working fluid was a 30% aqueous solution of KOH electrolyte with the following physical properties: the coefficient of kinematic viscosity $\nu = 2.1 \cdot 10^{-7}$ m^2/sec, density $\rho = 1.29 \cdot 10^{-3}$ kg/m^3, and specific electrical conductivity $\sigma = 54.34\ \Omega^{-1} \cdot m^{-1}$.

The channel was positioned between the poles of a direct-current magnet, producing a uniform magnetic field with induction B to 1.4 T. A current with a strength of I = 1-6 A and a density of **j** was passed with the aid of a direct-current source in the area between the electrodes. The interaction of the external magnetic field **B** with the current **j** flowing through the fluid leads to the appearance of a horizontal electromagnetic force $\mathbf{j} \times \mathbf{B}$ (see Fig. 1). Under the action of electromagnetic force the fluid is set into motion until equilibrium is established at the free surface of the fluid between the electromagnetic force and the force of gravity. The stationary initial profile of the free fluid surface is illustrated in Fig. 1.

This method makes it possible to alter the magnitude of the initial difference D in levels (Fig. 2) and the length L of the raised portion of the initial profile, as well as to set up a vortex pair in the area between the end wall and the electrodes. The change in the magnitude of the difference D is achieved by varying the current strength, and the change in the length L by displacement of the electrodes. The current strength and the position of the electrodes do not qualitatively change the shape of the stationary initial fluid profile. When the electrodes are positioned vertically no vortex pair is observed (see Fig. 2a, b). When the electrodes are slightly inclined ($\alpha = \pm 10°$) a stationary vortex pair is formed (see Fig. 2b, c). The formation of the vortices is governed by the nonuniformity of current discharge, which generates a moment of electromagnetic force relative to the horizontal axis. The direction of vortex rotation changes as electrode inclination is altered (see Fig. 2b, c). The angular velocity of the vortices

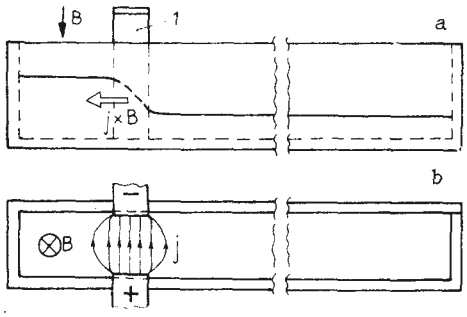

Fig. 1. Formulation of the initial fluid free-surface profile by the MHD method: side view (a) and top view (b).

Translated from Magnitnaya Gidrodinamika, Vol. 28, No. 1, pp. 65-72, January-March, 1992. Original article submitted June 21, 1991.

0024-998X/92/2801-0057$12.50

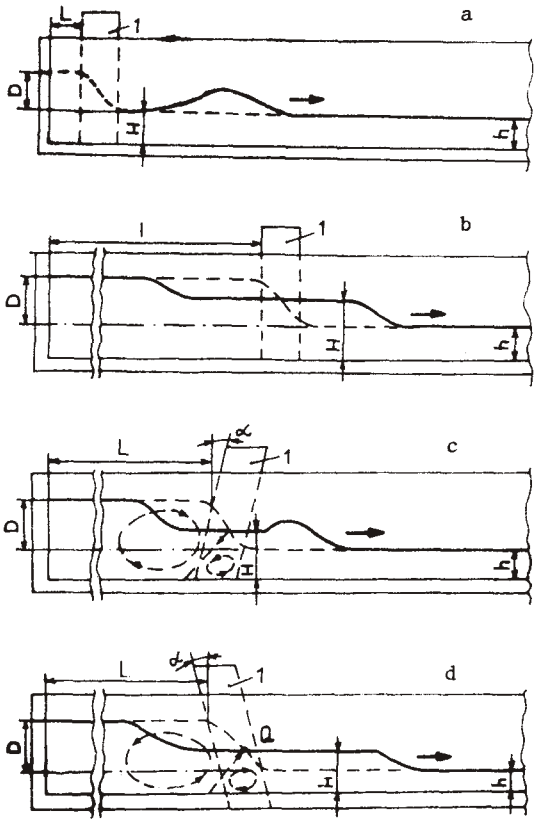

Fig. 2. Using the MHD method to generate solitary soliton waves (a), KdV bore waves (b), a truncated soliton wave (c), and an upper truncated KdV wave (d).

is determined by the current strength. The presence of a vortex pair has virtually no effect on the shape of the stationary initial profile of the fluid surface.

The formation of a solitary wave is concluded after the sudden switching off of the current. The influence of MHD effects on the propagation of the solitary wave is insignificant, since the electrical conductivity of the employed fluid is small and Ha << 1. The shape of the front in the solitary wave can be varied by displacement and inclination of the electrode, as well as by changing the current strength.

The described method of generating solitary waves can be used for an arbitrary fluid depth. In the present study it is used to generate solitary waves in shallow water. To prove the agreement between the experimental conditions and the conditions of shallow-water wave propagation, minute particles are placed at the bottom of the channel. In the propagation of a solitary wave the particles at the front of the wave are set into motion. Observation of the generated solitary waves bears out the two-dimensionality of their shapes.

The entire set of experimental conditions was tested in the process of generating a Korteweg—de Vries (KdV) wave [5, 6]. The basic diagram of soliton generation is shown in Fig. 2a, and the photograph of soliton propagation is shown in Fig. 3a. To produce a soliton the length L was chosen so that the fluid volume in the region DL of generation was commensurate with the volume of the soliton. The initial difference in levels coincided virtually with the amplitude A of the soliton, equal to 0.5 cm. The depth of the fluid did not exceed 0.25λ, where λ is the experimental wavelength, and amounted to about 4A. The formation of the soliton was completed at a distance of $l \leq 50A$. Reduction in l approximately by half in comparison to the data of other authors [1, 2] was governed by the low level of perturbations in the initial fluid profile. The shape of the solitary wave is determined with the aid of a procedure, described below, to process the photographs. Deviation in experimental shape of the soliton from the theoretical, described by the square of the secant [see (7)], did not exceed the experimental error (Fig. 4).

The basic diagram for bore generation on the basis of the KdV equation (KdV bore) is shown in Fig. 2b, and the photograph of bore propagation is shown in Fig. 3b. In the process of bore generation the length L was chosen so that the fluid volume in the generation region (D — H)L is commensurate with the bore volume $H(L_0 - L)$. The level D was greater by a factor of 2.5-3 than the bore amplitude $A = H - h \approx 0.5\text{-}0.7$ cm; here $h \approx 2.5A$. The level H was kept constant by the reserve

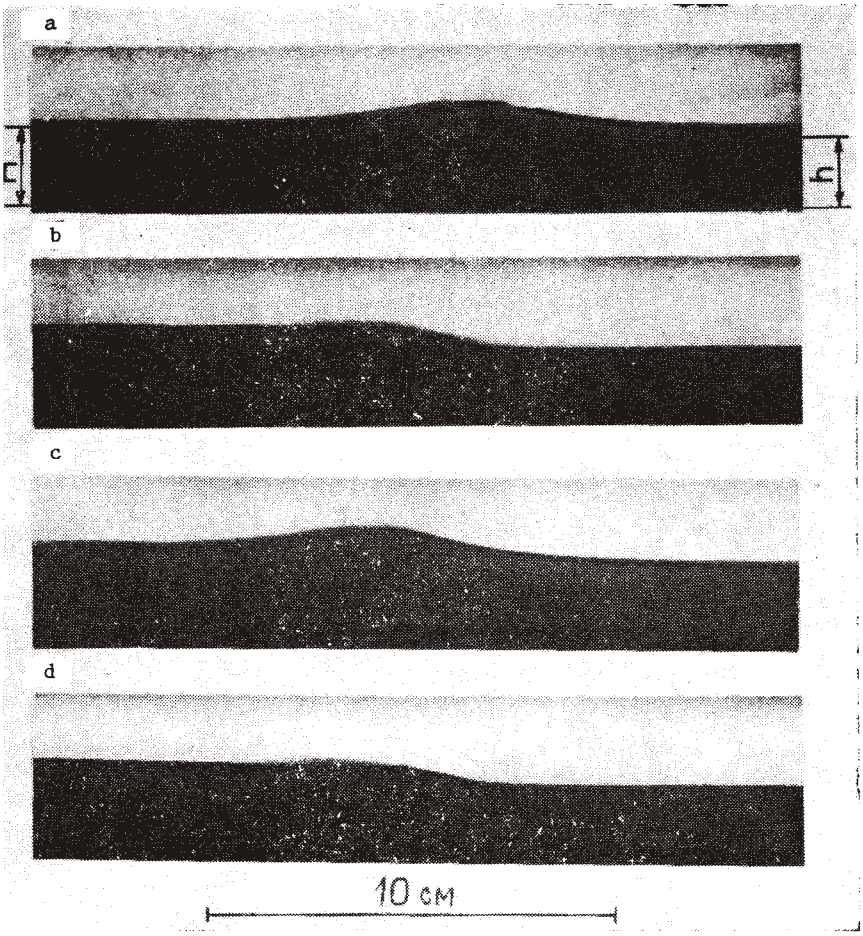

Fig. 3. Photographs illustrating the shape of propagating solitary waves: that of a soliton, h = H (a); that of KdV bore, h < H (b); that of a truncated soliton, h < H (c); and that of an upper truncated KdV bore, h < H (d).

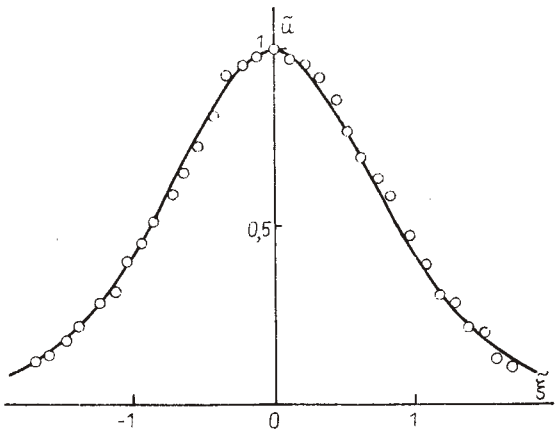

Fig. 4. The soliton in dimensionless coordinates: solid line) theory (1); o) experiment. The soliton at a distance of 27 cm from the electrodes.

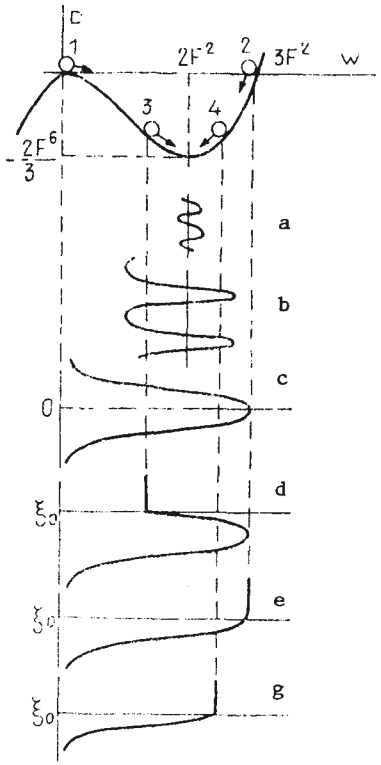

Fig. 5. Potential curve and various types of finite conserved motions of the system in the phase potential field (5): a) sinusoidal wave; b) cnoidal wave; c) soliton; d) truncated soliton; e) KdV bore; f) upper truncated KdV bore.

fluid at the D + h level. The described generation scheme is similar to that involving a barrier [3, 4], but as in the case of the soliton, the length of bore formation $l \leq 40A$ was reduced by half in comparison to [3, 4].

The possibility of establishing a vortex pair made it possible to generate bores with a different front shape. The schemes for the generation of such bores are shown in Fig. 2c, d, and their photographs can be seen in Fig. 3c, d. At the instant that the current is shut off the vortex pair produces a jet which in the vicinity of point Q changes the process of fluid overflow from the D + h level to the H level. After the shutting down of the current the vortices rapidly dissipated. The shape of the bore front depended on the direction of vortex rotation. The angular velocity of the vortices was on the order of 6 rad/sec for the case shown in Figs. 2c, 3c, and 10 rad/sec in the case of Figs. 2d and 3d. The parameters L, D, and h were chosen in the same way as for the generation of the bore shown in Figs. 2b and 3b. The length l of formation did not exceed 40A.

The Theoretical Model

To represent the bores obtained experimentally we employed the theory of solitary KdV waves in generalized functions. We used one of the solutions [7] found in the class of continuous functions with a discontinuity point $\xi = \xi_0$ of the first kind:

$$u = \left(S - F^2 + 3F^2 \operatorname{sech}^2 \frac{F}{2} \xi_0\right) \theta_- + \left(S - F^2 + 3F^2 \operatorname{sech}^2 \frac{F}{2} \xi\right) \theta_+. \tag{1}$$

Here u describes the shape of the wave; $\xi = x - St$ is a self-similar coordinate; the parameters S, F, and ξ_0 are used to determine the velocity, amplitude, and shape of the wave; θ_- and θ_+ are Heaviside functions:

$$\theta_- = \begin{cases} 0 \text{ for } \xi > \xi_0; \\ 1 \text{ for } \xi \leqslant \xi_0; \end{cases} \quad \theta_+ = \begin{cases} 1 \text{ for } \xi \geqslant \xi_0; \\ 0 \text{ for } \xi < \xi_0. \end{cases}$$

This solution satisfies the equation of KdV solitary waves in the generalized sense:

$$\int_{-\infty}^{\infty} [-Su'(\xi) + u(\xi)u'(\xi) + u'''(\xi)] \varphi(\xi) \, d\xi = 0,$$

where the basic function $\varphi(\xi)$ belongs to the fundamental space of infinitely differentiable functions with a compact carrier. The mathematical sense of the solution (1) is as follows: if the shape of the generated wave is described by a continuous function with a discontinuity point of the first kind and if at the point of discontinuity of the derivatives certain relationships are satisfied, then such a wave will propagate without change in shape.

Let us examine the physical sense of the solution (1). The problem of the solitary KdV wave in the general sense is described by the following ordinary differential equation [6]:

$$-Su'(\xi)+u(\xi)u'(\xi)+u'''(\xi)=0. \tag{2}$$

The transformation $v(\xi) = u(\xi) - S$ makes it possible to eliminate S from Eq. (2); thus, the following is valid for any wave velocity:

$$v(\xi)v'(\xi)=-v'''(\xi). \tag{3}$$

Equation (3) demonstrates the cause of solitary-wave shape constancy, namely equilibrium between nonlinearity and dispersion. Integration of (3) and substitution of $w(\xi) - F^2$ in the place of $v(\xi)$

$$\begin{aligned}\frac{d^2w}{d\xi^2}&=wF^2-\frac{w^2}{2};\\ \frac{d^2q}{d\tau^2}&=-\frac{1}{\mu}\frac{dP}{dq}\end{aligned} \tag{4}$$

show that the original problem (2) reduces to a problem of the conserved motion of a system with one degree of freedom in the potential field P of linear and quadratic forces [8]. The quantity w corresponds to the generalized coordinate q, while ξ corresponds to time τ. The subsequent integration of (4) yields the law of conservation of energy E:

$$\frac{w'^2}{2}+P(w)=E;\qquad P(w)=-\frac{F^2}{2}w^2+\frac{1}{6}w^3. \tag{5}$$

Figure 5 shows the graph of the potential energy. It should be pointed out that on integration of (3) the constant $F^4/2$ must be made positive. Otherwise the curve of the potential energy will have no equilibrium points and the finite motions in such a potential field will be impossible. The asymmetry of the potential well that is characteristic of many physical problems is a result of interaction between "repulsing" cubic and "attracting" quadratic potentials.

If the energy of the system near the bottom of the potential well $w = 2F^2$ differs little from the potential energy at this point $P(2F^2) = -2F^6/3$, the system will execute small symmetrical harmonic oscillations $W = w - 2F^2$ (see Fig. 5a), since the potential curve

$$P(w)=-F^2(2F^2+W)^2+(2F^2+W)^3/6$$

as $W \to 0$ tends toward a parabola:

$$P(w)\,|_{W\to 0}=-2F^6/3+F^2W^2/2. \tag{6}$$

With an increase in the energy of the system the oscillations in the ξ, W plane become asymmetric and cnoidal (see Fig. 5b). The potential energy (5) of the KdV problem (2) differs from potential energy (6) of any linear problem by the presence of the following (cubic) term in the expansion of the potential energy into a Taylor series. Owing to this fact we can explain the extensive area of application for KdV, since they are usually the result of the asymptotic expansions of initial nonlinear equations.

The search for solitary waves indicates from the physical standpoint a search for finite aperiodic motions of a system. Such a motion arises when a system acquires an energy $E = E_{max}$ equal to the potential energy $P = 0$ at the point of the local maximum $w = 0$. Integration of the law of the conservation of energy (5) then reduces to tabulated integrals, and the oft-cited expression for the KdV soliton is derived [9]:

$$w=u-S+F^2=3F^2\operatorname{sech}^2\frac{F}{2}\xi. \tag{7}$$

The KdV soliton is formed in the ξ, w plane (see Fig. 5c) for the case in which the system begins to move out of the local maximum $w = 0$ (point 1) at the instant $\xi = \xi_0 = -\infty$. It then rises to point 2 ($w = 3F^2$) when $\xi = 0$ and returns to point 1 when $\xi = \infty$. How can the system begin its motion away from point 1 if its initial velocity is equal to zero in accordance with (5), $dw/d\xi = 0$? The answer is as follows. The potential energy forms the surface in phase space (P, ξ, w), i.e., $P = P(\xi, w)$. For

simplicity Fig. 5 shows only the transverse cross section of this surface for some arbitrary ξ. The system begins to move along the ξ axis. In this case the initial velocity in the direction ξ, $d\xi/dw$, will be infinite, thus making it possible for the system to move from the local maximum. Naturally, at any instant of time different from the original, the quantity $d\xi/dw$ is finite.

Depending on the initial coordinate and velocity, we can cite three possible types of system motion in a potential well with energy E_{max} [10]. If the system begins its motion at $\xi = \xi_0$ out of point 3 (see Fig. 5) and the initial velocity is directed away from the local maximum, the projection of the motion onto the (ξ, w) plane (see Fig. 5d) will form a straight line $w = w(\xi_0)$ with $\xi < \xi_0$, which will change into a curve describing the greater portion of the KdV soliton when $\xi > \xi_0$. We can refer to a solitary wave of this type as a truncated soliton. If the system begins to move at $\xi = \xi_0$ out of point 2 ($w = 3F^2$) the projection of the motion (see Fig. 5e) will be a straight line $w = w(\xi_0)$ for $\xi < \xi_0$, which will change smoothly into half the soliton with $\xi > \xi_0$. Such a kink-like solitary wave can be referred to as a KdV bore. If the system begins its motion at $\xi = \xi_0$ out of point 4 and the initial velocity is directed away from the local maximum, the projection of the motion (see Fig. 5f) will be the line $w = w(\xi_0)$ with $\xi = \xi_0$, and this will change into a curve describing the smaller portion of the KdV soliton with $\xi > \xi_0$. Such a solitary wave can be referred to as an upper truncated KdV bore.

The physical sense of the solution (1) is thus associated with the conserved motion of a system with energy $E = E_{max}$ in the phase potential field (5). If at the initial instant of time $\xi = \xi_0$ the system, which is situated on the potential curve at the point $w_0 = w(\xi_0)$, acquires the velocity $(w')_0$ and acceleration $(w'')_0$, defined by relationships (5) and (5) for $E = E_{max}$

$$(w'')_0 = w_0 F^2 - \frac{w_0^2}{2}; \qquad (w')_0 = \pm \left[2 \left(\frac{F^2}{2} w_0^2 - \frac{1}{6} w_0^3 \right) \right]^{1/2}, \tag{8}$$

then the trajectory of its motion in the phase space (P, ξ, w) will coincide with the soliton trajectory (7) when $\xi > \xi_0$. With $\xi < \xi_0$

$$w = w_0; \qquad w'' = 0; \qquad w' = 0.$$

The described motion of the system corresponds to the solution (1), since $u = w + S - F^2$ is a continuous function, and the finite discontinuities in the derivatives coincide with the discontinuities in [7].

The shape of the solitary waves in the experiments was determined by processing of the photographs. For image contrast the working fluid was stained black by using a highly dispersed powder of activated carbon. Figure 3 only illustrates the solitary waves produced in the experiment. The processing of the photographs was carried out after a fourfold enlargement of the negative. The fact that the lines on the free surface of the fluid are blurred at certain spots in Fig. 3 is associated with the wettability of the channel walls by the electrolyte. The error in the determination of wave shape did not exceed 10%. The experimental points were plotted onto the graph in dimensionless coordinates $\tilde{u} = (u - h)/A$, $\tilde{\xi} = \alpha\xi/h$. The parameter α was determined by the method of least squares, using the dimensionless form of the solution (1):

$$\tilde{u} = \tilde{u}_0 \theta_- + \operatorname{sech}^2 \tilde{\xi} \theta_+,$$

where $\tilde{u}_0 = (H - h)/A$. Comparison of the experimental data against the theoretical curve (1) is shown in Fig. 6, where $\tilde{u} = \tilde{u}_0$ at point M. The constancy of the wavelength was maintained at distances from 40 to 60 A. These distances are shown in centimeters in Fig. 6a-c. Further observations of wave propagation were limited by channel length. The experimental and theoretical shapes of the waves coincided within the limits of experimental error, including the point M of derivative discontinuity.

Formation of a point of derivative discontinuity is related to processes which occur considerably more rapidly than the process of solitary wave propagation [11]. The theory [7] is based on the delta-function concept which simulates instantaneously occurring processes. High-speed processes developed in the experiment after the sudden shutting down of the current. Thus, for the KdV bore, at the instant of current cutoff, the equilibrium between the electromagnetic force and the force of gravity was disrupted and only the force of gravity continued to act on the fluid. Thus, acceleration of the initial free-surface profile was altered by a jump from 0 to $g \sin \gamma$, where g represents the acceleration of gravity and γ is the angle of free-surface inclination. At this instant the velocity of the free surface remained constant and equal to zero.

The described situation corresponds to the onset of system motion away from point 2 (see Fig. 5e), where $(w'')_0 \neq 0$ and $w_0 = 0$ in accordance with (8). In the experiment the constancy of the phase energy E was maintained by the constant difference D of levels (see Fig. 2b). The potential energy of the force of gravity was converted into the kinetic energy of the fluid flowing from the D + h level to the H level. The constancy of the H level corresponds in the theory to the initial coordinate of system motion $w_0 = w(\xi_0)$, which is a constant. The H level is experimentally maintained constant.

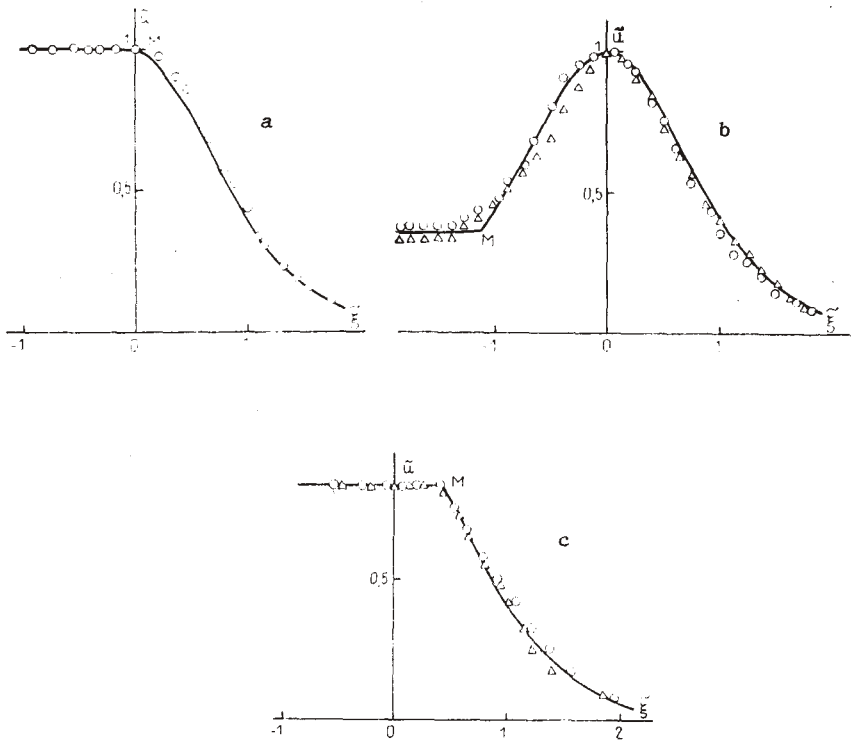

Fig. 6. Truncated soliton (a), KdV bore (b), and upper truncated KdV bore (c) in dimensionless coordinates. The curve represents theory (1); the points denote experiment: a) truncated solitons at distances of 27.5 (o) and 40 cm (Δ) from the electrodes; b) KdV bore at a distance of 26 cm from the electrodes; c) upper truncated KdV bores at distances of 36 (o) and 40 cm (Δ) from the electrodes.

In the case of a truncated soliton and an upper truncated KdV bore the discontinuity in the acceleration of the initial profile $(w'')_0 \neq 0$ arises analogously to the case of the KdV bore. The velocity of the free surface in the vicinity of point Q (see Fig. 2c, d) also changed discontinuously, owing to the inertia of the vortex pair generating the jet $(w')_0 \neq 0$. On transition from the generation of a truncated soliton to the generation of an upper truncated bore this velocity changed direction by 180°, since the direction of vortex rotation also changed. The change in direction for velocity corresponded in theory to the change in sign for $(w')_0$ in Eq. (8). The angular velocity and acceleration of free fall are finite in magnitude; therefore, the discontinuities in velocity $(w')_0$ and acceleration $(w'')_0$ for the system were also finite. Thus, the processes proceeding at high speed on sudden disconnection of the current made it possible, in the experiment, to generate solitary KdV waves corresponding to theoretical waves from the point of discontinuity of the first kind.

CONCLUSION

An MHD method is proposed in this study for the generation of solitary waves. In comparison with familiar methods, this procedure allows us to reduce the generating perturbations and thus to reduce by a factor of two the length of solitary wave formation. Through the use of this method we were able to generate new solitary KdV waves, a truncated soliton, a KdV bore, and an upper truncated KdV bore. The mechanism of their generation is discussed in conjunction with a model of conserved system motion in the phase potential field.

LITERATURE CITED

1. H. Segur and J. L. Hammack, "Soliton models of long internal waves," *J. Fluid Mech.*, **118**, 285-304 (1982).
2. M. Ablowitz and H. Segur, *Solitons and the Inverse Method* [Russian translation], Mir, Moscow (1987).
3. T. W. Kao, F.-S. Pan, and D. Renouard, "Internal solitons on the pycnocline: generation, propagation, and shoaling and breaking over a slope," *J. Fluid Mech.*, **159**, 19-53 (1985).
4. H. H. Yen and K.-M. Mok, "On turbulence in bores," *Phys. Fluids*, **2**, No. 5, 821-828 (1990).

5. R. Todd, J. Eilbeck, J. Gibbon, and H. Morris, *Solitons and Nonlinear Equations* [Russian translation], Mir, Moscow (1988).
6. G. Lamb, *Introduction to the Theory of Solitons* [Russian translation], Mir, Moscow (1983).
7. V. A. Miroshnikov, "Propagation theory of nonlinear solitary waves of the generalized KdV equation," in: Abstracts of Intern. Workshop: Waves and Vortices in the Ocean and Their Laboratory Analogs, Vladivostok (1991).
8. L. D. Landau and E. M. Lifshits, *Mechanics* [in Russian], Nauka, Moscow (1965).
9. M. Todd, *The Theory of Nonlinear Grids* [Russian translation], Mir, Moscow (1984).
10. Yu. B. Kolesnikov and V. A. Miroshnikov, "The completeness of the KdV bore system," in: Abstr. of Intern. Workshop: Anistropy of Fluid Flows in External Force Fields and Geophysical, Technological, and Ecological Applications, Jurmala (1990), p. 32.
11. V. Ketch and P. Teodorescu, *Introduction to the Theory of Generalized Functions and Their Applications in Engineering* [Russian translation], Mir, Moscow (1978).